Group B *Streptococcus* pilus sortase regulation: a single mutation in the lid region induces pilin protein polymerization *in vitro*

Roberta Cozzi,*,[1] Francesca Zerbini,*,[1] Michael Assfalg,† Mariapina D'Onofrio,† Massimiliano Biagini,* Manuele Martinelli,* Annalisa Nuccitelli,* Nathalie Norais,* John L. Telford,* Domenico Maione,*,[2] and C. Daniela Rinaudo*

*Novartis Vaccines and Diagnostics, Siena, Italy; and †Nuclear Magnetic Resonance Laboratory, Department of Biotechnology, University of Verona, Verona, Italy

ABSTRACT **Gram-positive bacteria build pili on their cell surface *via* a class C sortase-catalyzed transpeptidation mechanism from pilin protein substrates. Despite the availability of several crystal structures, pilus-related C sortases remain poorly characterized to date, and their mechanisms of transpeptidation and regulation need to be further investigated. The available 3-dimensional structures of these enzymes reveal a typical sortase fold, except for the presence of a unique feature represented by an N-terminal highly flexible loop known as the "lid." This region interacts with the residues composing the catalytic triad and covers the active site, thus maintaining the enzyme in an autoinhibited state and preventing the accessibility to the substrate. It is believed that enzyme activation may occur only after lid displacement from the catalytic domain. In this work, we provide the first direct evidence of the regulatory role of the lid, demonstrating that it is possible to obtain *in vitro* an efficient polymerization of pilin subunits using an active C sortase lid mutant carrying a single residue mutation in the lid region. Moreover, biochemical analyses of this recombinant mutant reveal that the lid confers thermodynamic and proteolytic stability to the enzyme.—Cozzi, R., Zerbini, F., Assfalg, M., D'Onofrio, M., Biagini, M., Martinelli, M., Nuccitelli, A., Norais, N., Telford, J. L., Maione, D., Rinaudo, C. D. Group B *Streptococcus* pilus sortase regulation: a single mutation in the lid region induces pilin protein polymerization *in vitro*. *FASEB J.* 27, 3144–3154 (2013). www.fasebj.org**

Key Words: transpeptidation · backbone protein · limited proteolysis · thermal stability · NMR spectroscopy

GROUP B *STREPTOCOCCUS* (GBS; *Streptococcus agalactiae*) is the leading cause of life-threatening diseases in newborns and is also becoming a common cause of invasive diseases in nonpregnant, elderly, and immune-compromised adults (1).

Pili have been discovered in several gram-positive pathogens, including GBS, as important virulence factors and potential vaccine candidates (2, 3). These long filamentous fibers protruding from the bacterial surface have been implicated in promoting phagocyte resistance and systemic virulence in animal models, in mediating attachment to human epithelial cells, and in biofilm formation (4–7).

S. agalactiae express 3 different 3-component pilus structures, in which multiple copies of a major protein subunit, also defined as backbone protein (BP), form the pilus shaft, and two accessory proteins, the major ancillary protein (AP1) and the minor AP (AP2) are located at the tip and at the base of the pilus, respectively, according to the current model of pilus assembly in gram-positive bacteria (8–11). AP1 typically functions as an adhesin, while AP2 is used as anchor subunit to covalently attach pili to the cell wall (12, 13). Structurally distinct pili are coded from 3 genomic islands, classified as pilus island 1 (PI-1), pilus island 2a (PI-2a), and pilus island 2b (PI-2b), each containing genes for the 3 structural components and at least 2 class C sortases that are directly involved in pilin subunit polymerization. Gene-knockout (KO) studies in *S. agalactiae* PI-1 and PI-2a, each expressing 2 sortases (SrtC-1 and SrtC-2), demonstrated that the deletion of

Abbreviations: 2D, 2-dimensional; AP, ancillary protein; BCA, bicinchoninic acid; BP, backbone protein; DSF, differential scanning fluorometry; ESI-QTOF MS, electrospray ionization–quadrupole time-of-flight mass spectrometry; FRET, fluorescence resonance energy transfer; GBS, group B *Streptococcus*; HMW, high molecular weight; HSQC, heteronuclear single quantum coherence; KO, knockout; MS, mass spectrometry; NMR, nuclear magnetic resonance; PDB, protein data bank; PI, pilus island; PIPE, polymerase incomplete primer extension; PMF peptide mass fingerprint; SDS-PAGE, sodium dodecyl sulfate–polyacrylamide gel electrophoresis; SEC, size-exclusion chromatography; SrtC, sortase C; TIGR, The Institute for Genomic Research; WT, wild-type

[1] These authors contributed equally to this work.

[2] Correspondence: Novartis Vaccines and Diagnostics, Via Fiorentina 1, 53100 Siena, Italy. E-mail: domenico.maione@novartis.com

doi: 10.1096/fj.13-227793

This article includes supplemental data. Please visit *http://www.fasebj.org* to obtain this information.

0892-6638/13/0027-3144 © FASEB

either sortase enzymes or the BP completely abrogated pilus polymerization (8, 9).

The pilus-associated sortases are membrane cysteine enzymes that build pili on the bacterial surface through a common transpeptidation mechanism involving specific motifs present in the monomeric precursors. They recognize and cleave the LPXTG sorting signal (where X denotes any amino acid) of the pilin proteins and covalently join the C terminus of one pilin subunit to a lysine side-chain NH_2 group on the next pilin (10, 14–17). However, while the catalytic mechanism of transpeptidation of the housekeeping sortase A (SrtA) is well characterized (18–22), more studies are required for a better understanding of substrate recognition specificity and regulation of class C sortase (23–26).

The available crystal structures of several pilus-related sortases, from *S. pneumoniae* (25, 27, 28), *Actinomyces oris* (29), *S. suis* (30), and GBS PI-1 (31–33) and PI-2a (34), have revealed that these enzymes contain a unique structural feature, a loop called the "lid," that hides the catalytic triad of the active site, folding the enzyme in a closed conformation. Moreover, this loop appears as a flexible region that could be displaced from the enzyme active site, suggesting an important role of the lid in enzyme activation, specifically in the regulation of substrate accessibility to the active site. The recently published atomic spatial coordinates of the C1 sortases from *S. suis* and GBS pilus type 1 in different space groups (*i.e.*, with the lid displaced from the active site) or in complex with a small-molecule cysteine protease inhibitor, provide further evidence that the lid is a mobile segment, and its displacement could result in an active site accessible to the substrate (30, 31). In agreement with these structural data, the crystal structure of the soluble domain of sortase C1 (SrtC1) from GBS PI-2a (SrtC1-2a) also shows that the catalytic triad composed of His157-Cys219-Arg228 is covered by the lid. Moreover, *in vivo* mutagenesis studies have clearly demonstrated that the catalytic triad is essential for pilus fiber formation, whereas the lid is dispensable. Finally, recombinant SrtC1 lid mutants perform even better than the wild-type (WT) enzyme in cleaving LPXTG-carrying peptides in *in vitro* assays (33–35). These structure-function relationships lead to the hypothesis that the catalytic activity of C sortases can be induced by the interaction with the substrate proteins and/or other unknown factors through a displacement of the lid from the active site of the enzyme.

In this work, we demonstrate that an efficient pilus protein polymerization can be obtained *in vitro* by using a recombinant SrtC1-2a lid mutant enzyme. By contrast, the WT enzyme was unable to polymerize the pilin backbone subunit *in vitro*. These data represent the first direct experimental evidence that these enzymes are autoinhibited by the presence of the lid and add new insights into the mechanisms of activity and regulation of pilus-associated class C sortases. Moreover, due to the key role of pili in bacterial virulence and pathogenesis, as well as their importance as promising vaccine candidates against GBS infections, the *in vitro* reconstruction of structurally complex polymers by using purified pilus subunits represents an amazing challenge, opening new perspectives for characterizing the pilus assembly mechanism through the use of activated forms of pilus-associated sortases.

MATERIALS AND METHODS

Bacterial strains and growth conditions

GBS 515 strain and mutants were grown in Todd-Hewitt broth (THB) or in trypticase soy agar (TSA) supplemented with 5% sheep blood at 37°C.

Cloning, expression, and purification of recombinant proteins

$SrtC1_{43-292}$ ($SrtC1_{WT}$), $SrtC1_{Y86A}$, carrying the substitution of Tyr86 into alanine and $SrtC1_{\Delta LID}$, containing the deletion of the entire lid region (residues 81–96), were expressed as His-MBP, TEV cleavable, fusion proteins (34). The mutant lacking the N-terminal domain, $SrtC1_{96-292}$ ($SrtC1_{\Delta NT}$), was generated by polymerase incomplete primer extension (PIPE) site-directed mutagenesis (36) using as template the WT HIS-MBP-$SrtC1_{43-292}$. The recombinant proteins were purified as described previously (34).

Genes coding for the pilus 2a BP_{30-649} (BP-2a) without the predicted N-terminal signal peptide and the C-terminal transmembrane domain, containing both the pilin motif and the sorting signal; and for BP_{30-640}, lacking the C-terminal IPQTG motif were PCR amplified from GBS strain 515, cloned in the speedET vector and expressed as N-terminal His-tagged, TEV cleavable, fusion proteins as described previously (37). The recombinant mutant BP_{K189A} was generated by PIPE site-directed mutagenesis using as template the WT BP_{30-649}. Protein purification was performed by immobilized-metal affinity chromatography (IMAC) followed by size exclusion using HiLoad 26/60 Superdex 200 (GE Healthcare; Life Sciences, Piscataway, NJ, USA) equilibrated in 25 mM Hepes and 75 mM NaCl (pH 7.5). The fractions containing the pure protein, which showed a single band on sodium dodecyl sulfate–polyacrylamide gel electrophoresis (SDS-PAGE), were quantified with the bicinchoninic acid (BCA) assay (Pierce; Thermo Scientific, Rockford, IL, USA).

In vitro polymerization assay

The *in vitro* polymerization assay was performed by mixing different concentrations of GBS $SrtC1_{WT}$ and $SrtC1_{Y86A}$ (1, 5, 10, 25, and 100 μM) and GBS BP-2a (25, 50, 100, and 200 μM). The volume of reaction was 50 μl in buffer containing 25 mM Tris-HCl, 100 mM NaCl, and 1 mM DTT (pH 7.5). DTT was added just to prevent the formation of potential disulfide bridges leading to aspecific SrtC1 dimerization during the incubation time. The incubation was performed at 37°C in a thermomixer, and the reaction was analyzed by SDS-PAGE at different time points (up to 3 d). The SDS-PAGE analysis was performed using 4–12% Criterion XT Bis-Tris Precast Gels (Bio-Rad, Hercules, CA, USA) with 2-(*N*-morpholino)ethanesulfonic acid (MES) running buffer and stained with Coomassie blue.

Differential scanning fluorometry (DSF)

The thermal stability of recombinant $SrtC1_{WT}$, $SrtC1_{\Delta LID}$, and $SrtC1_{Y86A}$ was investigated by DSF analysis. In a 96-well plate (Thermo-Fast 96-ABgene; Thermo Scientific), 40 μl of each sample containing 25 μM of the enzyme and 5× Sypro Orange (Sigma-Aldrich, St. Louis, MO, USA) in 25 mM Tris-HCl and 100 mM NaCl (pH 7.5) buffer was analyzed. The unfolding profile and the melting temperature were monitored by a quantitative PCR thermocycler (Stratagene, La Jolla, CA, USA) as already reported (38).

Antisera

Antisera specific for the BP-2a, AP1-2a, and AP2-2a proteins were produced by immunizing CD1 mice with the purified recombinant proteins, as described previously (2, 37).

Generation of complementation vectors

The complementation vector pAM_BP, in which BP-2a gene [The Institute for Genomic Research (TIGR) annotation SAL_1486], amplified from the GBS 515 genome, was cloned into the *Escherichia coli*-streptococcal shuttle vector pAM401/gbs80P+T and GBS-KO mutant strain for BP-2a protein (515ΔBP-2a) were generated as previously reported (9). The complementation vectors $pAM\_BP_{\Delta IPQTG}$ and pAM_BP_{K189A} were generated by PIPE site-directed mutagenesis (36) using pAM_BP vector as template for the introduction and/or deletion of specific mutations. Electrocompetent GBS-KO mutant cells (515ΔBP-2a) were transformed with the complementation vectors pAM_BP_{WT}, $pAM\_BP_{\Delta IPQTG}$, and pAM_BP_{K189A}. Complementation was confirmed by checking BP-2a expression by Western blotting.

Western blot analysis

Midexponential-phase bacterial cells were resuspended in 50mM Tris-HCl containing 400U of mutanolysin (Sigma-Aldrich) and Complete protease inhibitors (Roche, Indianapolis, IN, USA). The mixtures were then incubated at 37°C for 1 h and cells lysed by 3 cycles of freeze/thawing. Cellular debris was removed by centrifugation and protein concentration was determined using BCA protein assay (Pierce). Total protein extracts (20 μg) were resolved on 3–8 or 4–12% NuPAGE gels (Invitrogen, Carlsbad, CA, USA) by SDS-PAGE and transferred to nitrocellulose. Membranes were probed with mouse antiserum directed against BP, AP1, and AP2 proteins (1:1000 dilution), followed by a rabbit anti-mouse horseradish peroxidase-conjugated secondary antibody (Dako, Glostrup, Denmark). Bands were then visualized using an Opti-4CN substrate kit (Bio-Rad).

Limited proteolysis assay

Sequencing-grade Trypsin (Promega, Madison, WI, USA) was dissolved in the buffer provided to a final concentration of 0.2 μg/μl and was activated for 10 min at 37°C. Next, 2 μg of trypsin and 200 μg of $SrtC1_{WT}$ and $SrtC1_{Y86A}$ were mixed in a final volume of 100 μl in buffer (25 mM Tris-HCl and 100 mM NaCl, pH 7.5). The reactions were incubated in thermomixer at 37°C. Samples were collected after 5, 10, 20, 30, 60, and 120 min; the proteolysis was then quenched by adding final 0.1% formic acid (v/v) and analyzed by SDS-PAGE.

Intact mass determination by electrospray ionization–quadrupole time-of-flight mass spectrometry (ESI-QTOF MS)

The trypsin digestion mixture was diluted in 0.1% formic acid. The acidified protein solutions were loaded onto a Protein MicroTrap cartridge (60–100 pmol; Michrom Bioresources, Inc., Auburn, CA, USA), desalted for 2 min with 0.1% formic acid at a flow rate of 200 ml/min and eluted directly into the mass spectrometer using a step gradient of acetonitrile (55% acetonitrile and 0.1% formic acid). Spectra were acquired in positive mode on a SynaptG2 HDMS mass spectrometer equipped with a *Z*-spray ESI source (Waters Corp., Milford, MA, USA). The quadrupole profile was optimized to ensure the best transmission of all ions generated during the ionization process.

Analytic size-exclusion chromatography (SEC)

$SrtC1_{WT}$ was subjected to limited proteolysis for 30 min at 37°C, using the same amount and ratio of trypsin described above. The digestion mix was promptly loaded in Superdex 75 10/300 (GE Healthcare) equilibrated with 25 mM Tris-HCl (pH 7.5) and 150 mM NaCl, at the flow rate of 0.8 ml/min. The chromatography was performed using a UV detector monitoring at 280 nm, and 0.2 ml/tube fractions were collected. The protein fractions, identified by the chromatogram peaks, were analyzed by SDS-PAGE. A Bio-Rad gel filtration standard (cat. No. 151–1901) was used for the calibration of standard peaks.

Nuclear magnetic resonance (NMR) spectroscopy

Fifteen nitrogen-labeled recombinant proteins were expressed growing bacteria in M9 minimal medium containing 1 mg/ml of $(^{15}NH_4)_2SO_4$ as a sole source of nitrogen and otherwise following the same protocols as for unlabeled samples. The protein buffers were exchanged using a PD-10 desalting column (Amersham Biosciences, Arlington Heights, IL, USA), equilibrated with 50 mM phosphate buffer (pH 6.5), and finally concentrated by ultrafiltration to ~0.2 mM. Next, ^{1}H-^{15}N heteronuclear single-quantum coherence (HSQC) spectra were recorded at 25°C on a Bruker Avance III spectrometer (Bruker, Karlsruhe, Germany) operating at 600.13 MHz proton Larmor frequency, equipped with a cryogenic probe. A standard ^{1}H-^{15}N HSQC pulse sequence was used, with pulsed field gradients for suppression of the solvent signal and cancellation of spectral artifacts. Next, 2048 (^{1}H) × 256 (^{15}N) complex data points were acquired with spectral windows of 9515.385 Hz (^{1}H) × 2432.718 Hz (^{15}N), 8 transients, and 1.2-s relaxation delay. Proton T_2 measurements were performed with the 1D oneone echo sequence (39) using variable delays of 0.2 and 5.2 ms and evaluating the corresponding signal intensities $[T_2 = 2 \times (5.2 - 0.2)/\ln(I_{0.2}/I_{5.2})]$. Processing of all the spectra was performed with Topspin2.1 (Bruker, Karlsruhe, Germany).

RESULTS

WT SrtC1-2a is not able to induce recombinant BP polymerization *in vitro*

The crystal structure of SrtC1 from GBS pilus 2a [SrtC1-2a; Protein Data Bank (PDB) ID 3O0P] shows that the catalytic cysteine (Cys219) is locked by the

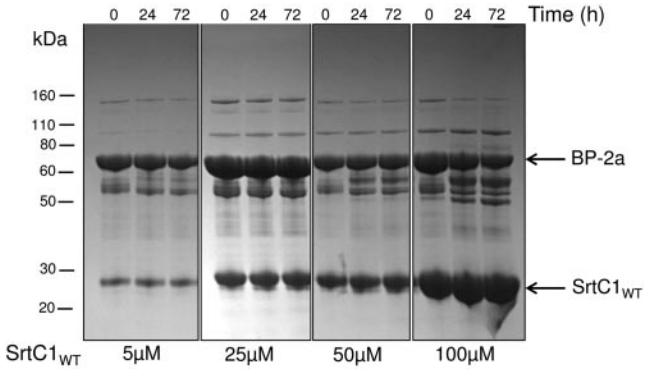

Figure 1. $SrtC1_{WT}$ is not able to polymerize the backbone subunit BP-2a *in vitro*. Time course of reactions with different concentrations (5, 25, 50, and 100 μM) of the WT SrtC1 enzyme ($SrtC1_{WT}$) mixed with a fixed concentration (100 μM) of the recombinant BP-2a. Aliquots of each reaction at different time points (0, 24, and 72 h) were separated by SDS-PAGE and Coomassie staining. No HMW structures have been identified in any sample.

aromatic ring of Tyr86 present in the lid, suggesting that this interaction maintains the enzyme in an inactive conformation (34).

To investigate the hypothesis that the presence of the lid covering the active site inhibits the catalytic activity of the enzyme, we tested the ability of the WT SrtC1-2a ($SrtC1_{WT}$) to polymerize the recombinant PI-2a BP (BP-2a). It is well-known that at least 2 components are necessary and sufficient for pili polymerization *in vivo*: the BP, forming the pilus shaft, and at least 1 SrtC coded by the same genomic pilus locus (9). The presence of covalently linked pili on the GBS surface can be detected by SDS-PAGE immunoblot analysis of cell-wall preparations through the identification of a ladder of high-molecular-weight (HMW) bands (9). Thus, we set up *in vitro* reactions in which different concentrations (5, 25, 50, and 100 μM) of purified recombinant $SrtC1_{WT}$ were mixed with a fixed concentration (100 μM) of the recombinant BP-2a and incubated at 37°C for up to 72 h. The reactions were analyzed by searching for a pattern of HMW bands by SDS-PAGE. In all the conditions used, no HMW bands were observed (**Fig. 1**). However, the presence of some bands at a higher molecular weight than that of the monomeric protein was detected. These bands, analyzed by MS, corresponded to the formation of a heterodimer formed by $SrtC1_{WT}$ and BP-2a and a BP-BP dimer (data not shown), whose formation was not promoted by the sortase since it was visible also in absence of $SrtC1_{WT}$ (Fig. 1 and Supplemental Fig. S1*A*). Identical results were obtained with different concentrations of BP-2a substrate (25, 50, 100, and 200 μM) incubated with a fixed amount of 25 μM of $SrtC1_{WT}$ (Supplemental Fig. S1*B*). These data suggest that the interaction between the WT form of SrtC1 and its BP-2a substrate is not alone sufficient to induce lid displacement from the catalytic pocket and to promote *in vitro* pilin subunit polymerization.

BP-2a HMW structures can be assembled *in vitro* by recombinant SrtC1 lid mutant

To investigate whether the mutant enzyme $SrtC1_{Y86A}$, in which the interaction between the catalytic cysteine and the Tyr 86 of the lid is abrogated, could be efficient in polymerizing BP-2a monomers in HMW structures, we repeated *in vitro* polymerization experiments using $SrtC1_{Y86A}$. Thus, 100 μM of the purified BP (BP-2a) was incubated at 37°C with the recombinant $SrtC1_{Y86A}$ mutant at different concentrations (5, 25, 50, and 100 μM). Samples from the single reactions were collected after 24, 48, and 72 h, treated with SDS, in a sample buffer containing also a reducing agent, and analyzed by SDS-PAGE. After Coomassie-staining, the formation of a typical pili pattern of bands corresponding to molecular weight above 260 kDa was observed in all reactions performed, also providing clear evidence of the covalent nature of the polymerized pilus structures (**Fig. 2**). We also observed that at the highest enzyme concentration, some of the BP-2a monomer remained unprocessed, and a complete conversion of monomeric BP-2a in polymeric structures could not be achieved (Fig. 2). Furthermore, the rate of recombinant BP polymer formation did not change even when different concentrations of the BP-2a substrate were used in the reaction, starting from 25 to 200 μM mixed with a fixed concentration (25 μM) of the enzyme (Supplemental Fig. S1*C*). However, in the presence of HMW polymeric structures, monomeric forms of the pilin subunits can always also be detected in total proteins prepared from GBS strains (9). Moreover, *in vivo*, the BP-2a polymerization process (9) is more efficient than the *in vitro* polymerization, as the HMW structures are of higher molecular weight than the polymers formed *in vitro* (Fig. 2).

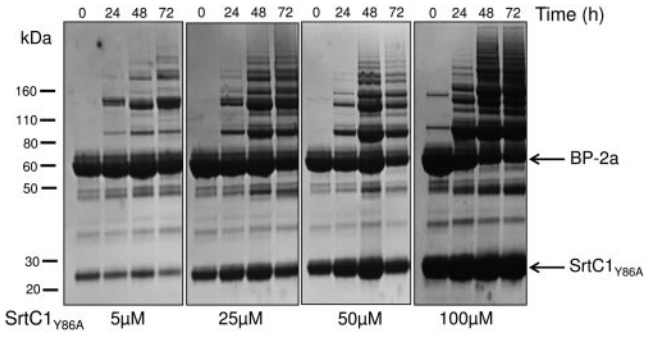

Figure 2. $SrtC1_{Y86A}$ polymerizes the backbone subunit BP-2a *in vitro*. Time course of reactions with different concentrations (5, 25, 50, and 100 μM) of the lid mutant enzyme carrying the substitution of Tyr86 into alanine ($SrtC1_{Y86A}$) mixed with 100 μM of the recombinant BP-2a. Samples (8 μl) of each reaction (8, 12, 20, and 36 μg of total proteins) at different time points (0, 24, 48, and 72 h) were analyzed by SDS-PAGE and Coomassie staining. A pattern of HMW bands has been detected in all the reactions analyzed.

Lys189 in the putative pilin motif and the IPQTG sorting signal of BP-2a are essential for pilus formation *in vivo*

To better characterize the HMW pilus-like structures obtained by polymerization of BP-2a monomers mediated by the $SrtC1_{Y86A}$ mutant, we investigated the role of specific residues/motives of the BP-2a sequence in pilus 2a polymerization. To identify these sequence elements, we first performed sequence comparisons of the homologous pilin subunits in different gram-positive bacteria. In the BP-2a sequence (strain 515, TIGR annotation SAL_1486) we identified a putative pilin motif containing a highly conserved lysine residue (Lys189), and the IPQTG motif in position 641–645 as the C-terminal sorting motif. To demonstrate the specific contribution in pilus assembly of both the Lys189 in the pilin motif and the IPQTG motif, we used site-specific mutagenesis and complementation studies.

The plasmid (pAM-BP_{K189A}) expressing a BP carrying a mutation of the pilin motif lysine residue into alanine and the second plasmid (pAM-$BP_{\Delta IPQTG}$) carrying a deletion of the entire IPQTG sorting signal were used to transform the GBS-KO mutant strain lacking the BP-2a gene (515ΔBP-2a) (9, 40). After complementation, the effects of each mutation/deletion on pilus formation were assessed by Western blot analysis, using total proteins extracted from each complemented strain and sera specific for the pilin subunits. As expected, both the K189 residue and the C-terminal IPQTG of BP-2a were absolutely required for pilin protein incorporation into the HMW structures *in vivo* (**Fig. 3**). When the K189 was mutated into an alanine, only the monomer form of the BP-2a could be identified, whereas when the sorting signal IPQTG was deleted in the BP-2a, in addition to the monomeric form of BP-2a, a higher-molecular-weight band was also observed. Immunoblot analysis performed with antibodies raised against the backbone subunit (α-BP) and the major ancillary pilin (α-AP1) showed that this higher-molecular-weight band, resistant to SDS treatment, contained both the BP and the major AP (AP1). Indeed, the polymerization of the BP-2a cannot occur as its sorting signal is deleted, but the pilin motif of the BP-2a is still available to form a covalent bond between the BP-2a pilin motif and the AP1-2a sorting signal (Fig. 3).

The IPQTG sorting signal is essential for the transpeptidation reaction mediated *in vitro* by the $SrtC1_{Y86A}$ mutant

To investigate the specific contribution of the Lys189 in the pilin motif and the IPQTG sorting signal in the *in vitro* polymerization reaction, we expressed in *E. coli* and purified mutated forms of the BP-2a protein, $BP_{\Delta IPQTG}$ and BP_{K189A}, carrying the deletion of the IPQTG region and the substitution of the Lys189 with an alanine, respectively. After mixing the active $SrtC1_{Y86A}$ with the recombinant $BP_{\Delta IPQTG}$ mutant,

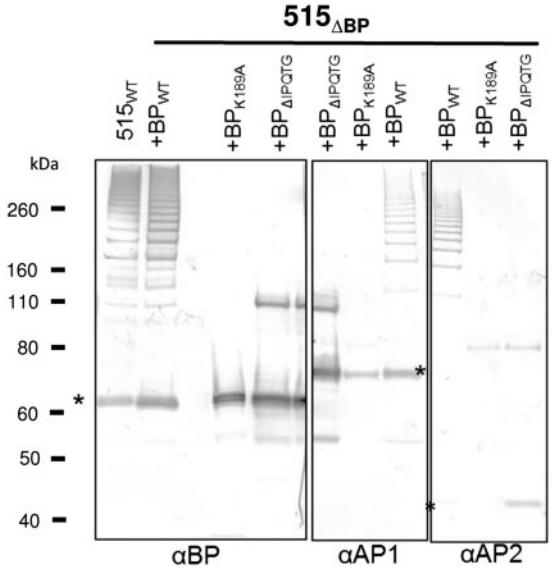

Figure 3. IPQTG motif and lysine 189 of BP-2a are essential for pilin subunit polymerization in HMW complexes in GBS strain 515. Western blot analyses of total protein extracts from the WT strain 515 (515_{WT}) and the deletion mutant strain for BP-2a ($515_{\Delta BP}$) complemented by plasmids expressing the WT BP gene (BP_{WT}) or the BP gene carrying the mutation K189A (BP_{K189A}) or the deletion of the IPQTG sorting motif ($BP_{\Delta IPQTG}$). Nitrocellulose membranes were probed with antisera specific for the BP (αBP) and the APs (αAP1 and αAP2).

HMW polymers could not be detected, confirming that the polymerization reaction occurs through the cleavage of the sorting signal and the formation of the acyl-intermediate between $SrtC1_{Y86A}$ and the IPQTG motif (**Fig. 4*A***). On the contrary, in the reactions in which the active $SrtC1_{Y86A}$ was incubated with BP_{K189A}, some oligomers could be observed, indicating that the Lys residue of the pilin motif (K189), conversely from what happens *in vivo*, is not essential for *in vitro* oligomerization (Fig. 4*B*). However, in the presence of BP_{K189A}, the formation of HMW structures *in vitro* did not appear so efficient if compared with those obtained using WT BP-2a. Moreover, when $SrtC1_{Y86A}$ was mixed with recombinant forms of the APs (AP1-2a and AP2-2a), which can be polymerized *in vivo* only in the presence of the BP-2a protein (34), some polymers were formed (Fig. 4*C*). These data suggest that to perform protein polymerization *in vitro*, $SrtC1_{Y86A}$ can use different nucleophiles to resolve the acyl intermediate between the enzyme and the LPXTG-like sorting signal.

Biochemical characterization of SrtC1-2a mutants reveals that the lid is involved in protein stability

To explore the effects of the lid anchoring residue Tyr86 and the entire lid region on the stabilization of SrtC1-2a enzyme, recombinant forms of $SrtC1_{WT}$, $SrtC1_{Y86A}$, and $SrtC1_{\Delta LID}$ (34) were studied by DSF. DSF is a technique used to monitor the thermal unfolding of proteins in the presence of a fluorescent dye

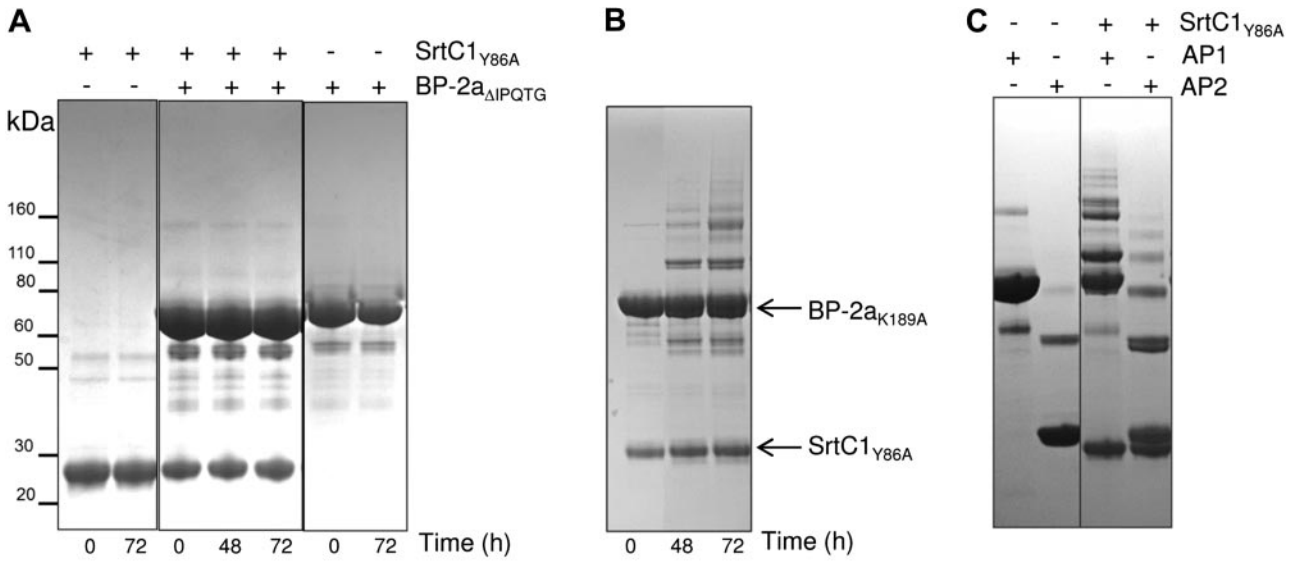

Figure 4. IPQTG motif of BP-2a is crucial for pilus polymerization *in vitro*. *A*) SDS-PAGE of the reactions between the lid mutant sortase ($SrtC1_{Y86A}$) and the recombinant mutant BP ($BP_{\Delta IPQTG}$) stopped at different time points (0, 48, and 72 h). The reactions were performed at 37°C using 25 μM of $SrtC1_{Y86A}$ and 100 μM of $BP_{\Delta IPQTG}$. No formation of HMW bands was detected. As negative controls, the $SrtC1_{Y86A}$ (on the left) and $BP\text{-}2a_{\Delta IPQTG}$ (on the right) were incubated alone in the same conditions. *B*) Lysine 189 of BP-2a pilin motif is not essential for *in vitro* pilus polymerization. $SrtC1_{Y86A}$ (25 μM) and recombinant BP_{K189A} (100 μM) were mixed at 37°C, and the reactions were analyzed by SDS-PAGE and Coomassie staining at different time points (0, 48, and 72 h). A weaker pattern of HMW structures could be identified. *C*) $SrtC1_{Y86A}$ can polymerize the pilus 2a APs AP1 and AP2, harboring the LPXTG-like sorting motif. $SrtC1_{Y86A}$ was incubated with the recombinant proteins AP1 or AP2; after 72 h, the reactions were analyzed by SDS-PAGE and Coomassie staining. Recombinant AP1 and AP2 proteins were incubated alone in the same conditions as negative controls.

(Sypro orange) that displays weak fluorescence in hydrophilic environments and becomes highly fluorescent in a hydrophobic environment, such as that provided by the exposed side chains of hydrophobic residues of an unfolded protein (38). The thermal denaturation curves, shown in **Fig. 5*A***, indicate that the melting temperature T_m for $SrtC1_{Y86A}$ is reduced by almost 10°C compared to that of the WT enzyme (52°C *vs.* 61°C). $SrtC1_{\Delta LID}$ shows an even lower T_m (47°C) and high pretransition baseline fluorescence suggestive of a partial exposure of the sortase hydrophobic core or partial aggregation.

The structural integrity of the produced mutants was verified by 2-dimensional (2D) NMR spectroscopy. ^1H-^{15}N HSQC spectra display signals for all backbone HN atoms in a 2D array defined by a proton and a nitrogen frequency dimension. Due to high sensitivity of peak positions to the proximal chemical environment of the corresponding atoms, a well-dispersed spectrum is characteristic of a folded protein. The ^1H-^{15}N HSQC peaks of both the $SrtC1_{WT}$ and $SrtC1_{Y86A}$ are distributed over a large spectral range (~5 ppm, ^1H, and ~30 ppm, ^{15}N; Fig. 5*B*), confirming the expected globular fold of the soluble domain, also in the presence of an extended transmembrane stretch at the C terminus. It can be observed that many of the isolated peaks have unchanged positions for $SrtC1_{Y86A}$ compared to $SrtC1_{WT}$; however, major perturbations in some areas of the spectrum are indicative of a non-negligible structural rearrangement, most likely affecting the lid region. Minor protein aggregation is suggested by the broader signals of the mutant, particularly in the center of the spectrum. The latter phenomenon was also analyzed and confirmed by measurement of the average transverse proton spin relaxation time T_2, a sensitive indicator of the overall tumbling rate of the molecule. The T_2 value for $SrtC1_{Y86A}$ was determined as slightly shorter compared to the WT protein. While the conformational transition induced by the Y86A mutation apparently preserves the overall enzyme fold, producing only localized conformational changes, the ^1H-^1D and the ^1H-^{15}N HSQC spectra (Supplemental Fig. S2) of the recombinant $SrtC1_{\Delta LID}$ mutant show largely broadened peaks with reduced frequency dispersion, indicative of protein aggregation, probably due to the exposure of the hydrophobic core covered by the lid in $SrtC1_{WT}$.

Lid anchoring to the active site led to an overall protection of SrtC1 from proteolysis

To investigate the differences in structural stability between the recombinant nonpolymerizing $SrtC1_{WT}$ and the polymerizing $SrtC1_{Y86A}$ mutant in solution, we probed the sensitivity of both proteins to limited proteolysis. Trypsin-SrtC1digestion was tested at different time points; the reaction was quenched by adding 0.1% formic acid and analyzed by SDS-PAGE. The observed digestion patterns of $SrtC1_{WT}$ and $SrtC1_{Y86A}$ were different, indicating that the two enzymes differ in susceptibility to proteolysis (**Fig. 6*A***). SDS-PAGE analysis of the proteolytic products indicated that $SrtC1_{WT}$ presented two predominant bands of digestion, approxi-

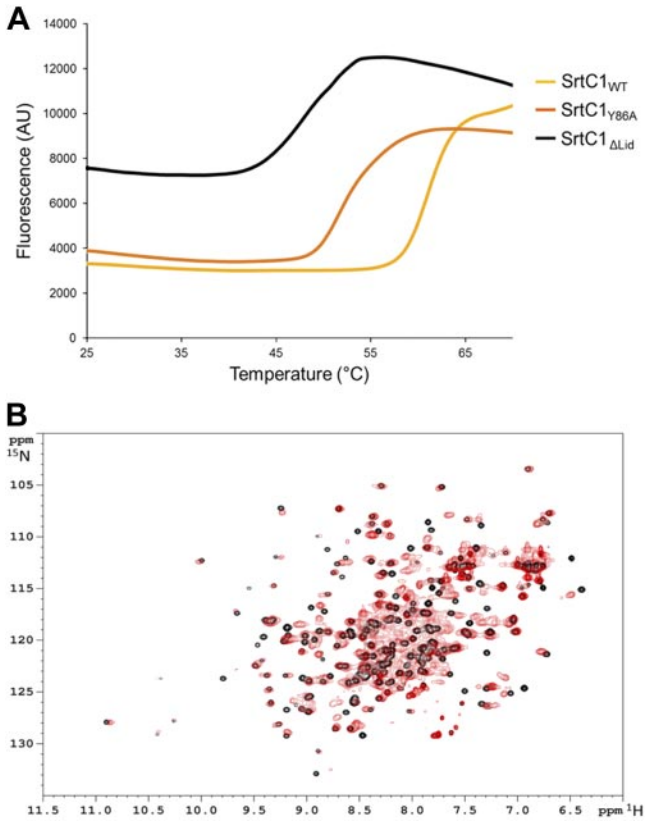

Figure 5. DSF and NMR analysis of $SrtC1_{WT}$ and mutants. *A*) DSF analysis of $SrtC1_{WT}$, $SrtC1_{Y86A}$, and $SrtC1_{\Delta LID}$ in presence of Sypro orange showed different thermal stabilities. Graph shows fluorescence intensity *vs.* temperature for the unfolding of $SrtC1_{WT}$, $SrtC1_{Y86A}$, and $SrtC1_{\Delta LID}$ in 25 mM Tris-HCl and 100 mM NaCl (pH 7.5). Melting temperatures of $SrtC1_{WT}$ (yellow trace), $SrtC1_{Y86A}$ (orange trace), $SrtC1_{\Delta LID}$ (black line) were 61, 52, and 47°C, respectively. *B*) Superimposed $^{1}H,^{15}N$-HSQC spectra of $SrtC1_{Y86A}$ (red) and $SrtC1_{WT}$ (black) enzymes. Signals of the residues in both proteins appear with a similar pattern, consistent with folded proteins.

mately at 17 and 6 kDa, respectively, still detectable after 60 min (Fig. 6*A*). On the contrary, the mutant $SrtC1_{Y86A}$ after only 10 min of trypsin digestion generated a series of fragments, including a fragment at around 17kDa that, however, was completely degraded after 20 min (Fig. 6*A*). Intact mass measurement by ESI-QTOF of the 5-min digestion mixture with $SrtC1_{WT}$ revealed that the most intense product of digestion contained 2 polypeptidic species, the most abundant of 16986.45 ± 0.54 Da (91–245 aa) and a less abundant of 16616.88 ± 0.47 Da (94–245 aa). The lowest-molecular-weight proteolysis product showed a mass of 6082.56 ± 0.54 Da (1–52 aa), corresponding to the N terminus of the recombinant WT SrtC1 (Fig. 6*B*). The residues of undigested SrtC1 were not detected in the ESI spectrum. The primary sequence obtained from intact measurement was also confirmed by peptide mass fingerprint (PMF) of SDS-PAGE bands (data not shown). Taken together, MS data showed that the trypsin cleavage site occurred around position 90, generating a fragment that is the N-terminal region of the sortase, including the lid residues, and an equimolar fragment that is the sortase β-barrel catalytic core (Fig. 6*C*). Therefore, the susceptibility to proteolytic attack of the catalytic β-barrel core was greatly increased in the mutant enzyme where Tyr86 was replaced with alanine, suggesting a role of the lid in providing enzyme stability and proteolysis resistance.

To better investigate whether the higher proteolytic resistance of $SrtC1_{WT}$ compared to $SrtC1_{Y86A}$ lid mutant was due to the interaction between Tyr86 and the catalytic C219 in the active site (an interaction that persists after the cleavage of the N-terminal region), we analyzed the $SrtC1_{WT}$-trypsin reaction mixture after 5 min of digestion by analytic SEC (**Fig. 7*A***). The fractions corresponding to major peaks were collected and analyzed by SDS-PAGE (Fig. 7*B*). Fractions 15 and 16 (predominant peak) contained both undigested $SrtC1_{WT}$ and 2 new bands, the proteolytic resistant fragment (17 kDa) and the N-terminal fragment (6 kDa). This result suggests that the lid still interacts with the catalytic cleft, contributing to the further resistance of the sortase core domain to digestion. The elution profile of the $SrtC1_{WT}$ enzyme alone by analytic SEC is reported in Supplemental Fig. S3.

By taking together the NMR, DSF, and proteolysis assays, it can be concluded that lid mutants, even when preserving a globular fold, sample open conformational states at lower energy compared to the WT protein, suggesting that the Tyr86-Cys219 interaction plays an important role in the thermodynamic and structural stabilization of SrtC1.

SrtC1 enzyme deleted of the entire N-terminal region is active in polymerizing BP *in vitro*

To investigate whether the sortase resistant core identified by MS is the minimal catalytic domain sufficient for sortase activity, a truncated construct, $SrtC1_{\Delta NT}$, containing only the core domain and deleted of the N-terminal region including the lid loop, was designed. Recombinant $SrtC1_{\Delta NT}$ was recovered with a lower yield than the WT enzyme; however, a sufficient amount was tested in the *in vitro* polymerization assay in comparison with $SrtC1_{WT}$ and $SrtC1_{Y86A}$. SDS-PAGE analysis of the reactions showed that $SrtC1_{\Delta NT}$ was able to polymerize the BP-2a, with a pattern of HMW structures similar to that obtained with the single lid mutant $SrtC1_{Y86A}$ (**Fig. 8**). These data suggest that the N-terminal domain is not essential for BP-2a polymerization *in vitro*, further supporting its regulatory function.

DISCUSSION

In this study, we provide novel insights into the mechanism of regulation and activation of pilin-associated class C sortases that build structurally complex pili on the surface of gram-positive bacteria. By using an *in vitro* assay, we demonstrate that an efficient polymerization of pilin proteins in HMW complexes can be

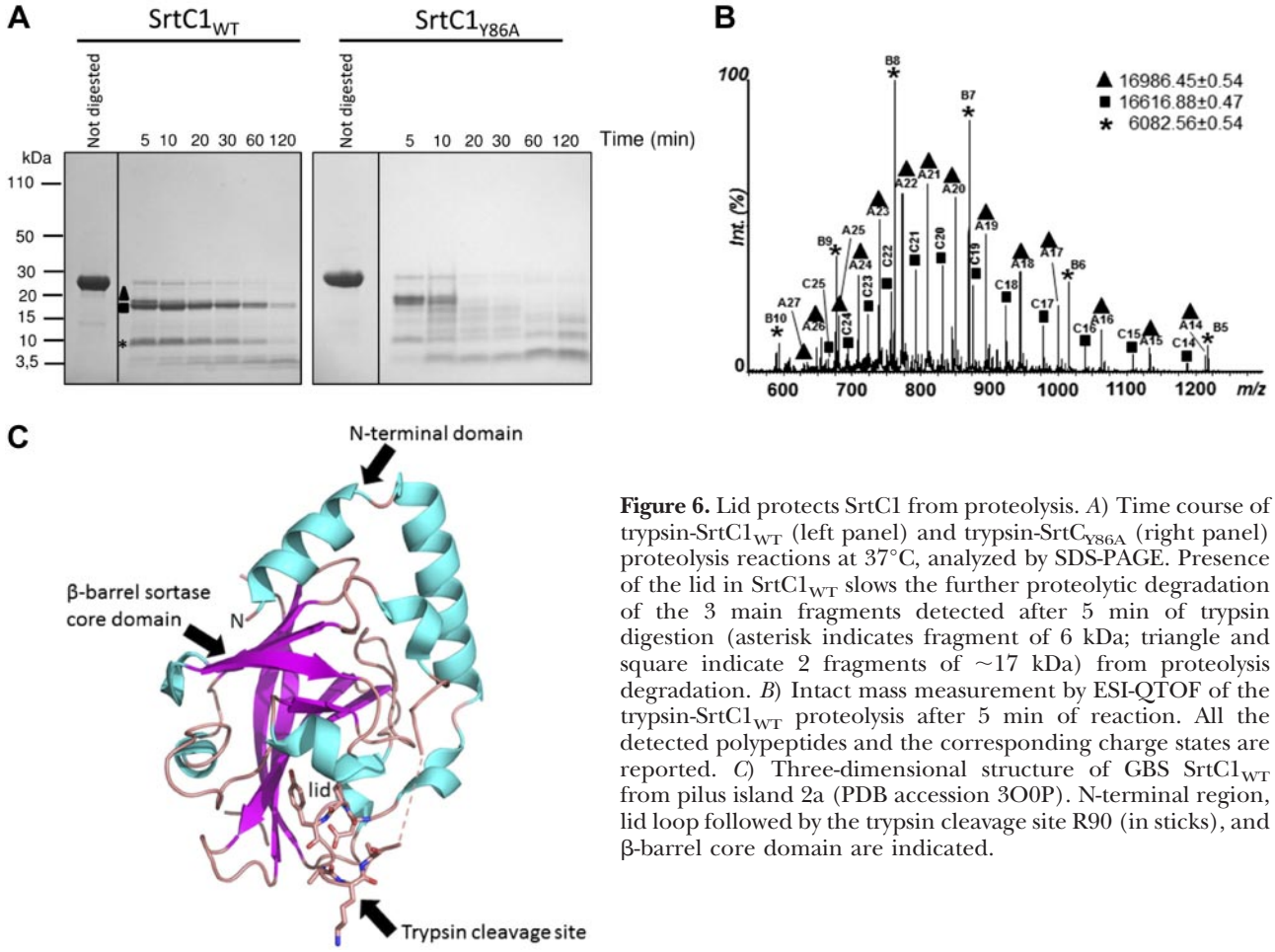

Figure 6. Lid protects SrtC1 from proteolysis. *A*) Time course of trypsin-SrtC1$_{WT}$ (left panel) and trypsin-SrtC$_{Y86A}$ (right panel) proteolysis reactions at 37°C, analyzed by SDS-PAGE. Presence of the lid in SrtC1$_{WT}$ slows the further proteolytic degradation of the 3 main fragments detected after 5 min of trypsin digestion (asterisk indicates fragment of 6 kDa; triangle and square indicate 2 fragments of ~17 kDa) from proteolysis degradation. *B*) Intact mass measurement by ESI-QTOF of the trypsin-SrtC1$_{WT}$ proteolysis after 5 min of reaction. All the detected polypeptides and the corresponding charge states are reported. *C*) Three-dimensional structure of GBS SrtC1$_{WT}$ from pilus island 2a (PDB accession 3O0P). N-terminal region, lid loop followed by the trypsin cleavage site R90 (in sticks), and β-barrel core domain are indicated.

achieved by using a recombinant sortase C lid mutant, expressed in soluble form and purified from *E. coli*. This mutant was generated based on structural analysis of the 3D structure of SrtC1-2a (34). The SrtC1-2a crystal structure showed that the aromatic ring of Tyr86 in the N-terminal lid region is positioned in a highly conserved hydrophobic environment (Leu131, Leu138, Val153, Leu217) and can potentially be involved in CH-π weak polar interactions with specific residues, including the catalytic Cys219 of the enzyme active site (34). This kind of interaction has been also observed in other pilus-related sortase structures, suggesting that the lid closes the active site contributing to an overall stability of the protein (27–29, 34). Starting from these

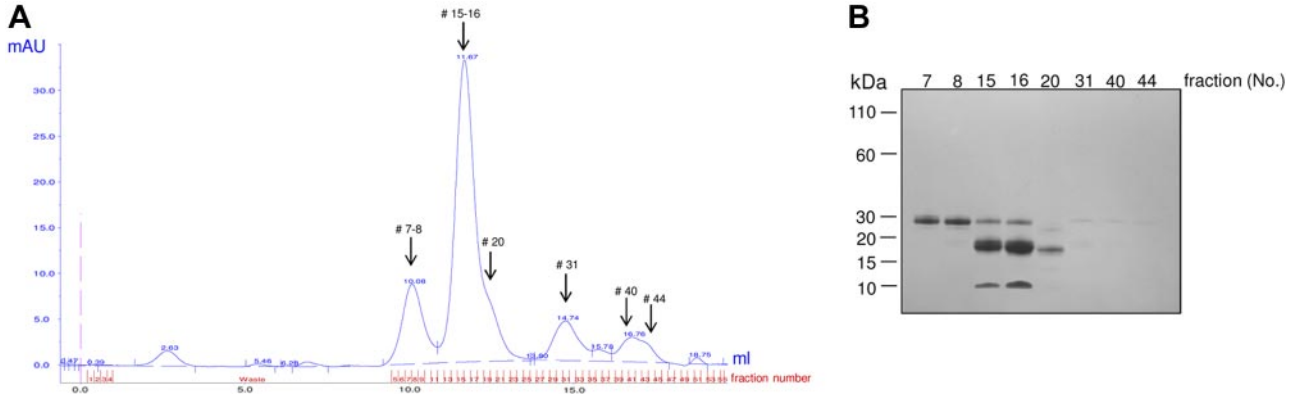

Figure 7. Interaction of the N-terminal domain with the sortase β-barrel core. *A*) SEC profile of the trypsin-SrtC1$_{WT}$ mixture. Digestion mixture of trypsin–SrtC1$_{WT}$ (ratio 1:100) in buffer (25 mM Tris-HCl and 150 mM NaCl) was loaded in a superdex75 10/300 column. Fractions corresponding to the major peaks (7, 8, 15, 16, 20, 31, 40, and 44 kDa) were collected and analyzed by SDS-PAGE. *B*) SDS-PAGE of the 8 fractions collected by SEC, showing the coelution of the N-terminal region and the sortase core of SrtC1$_{WT}$.

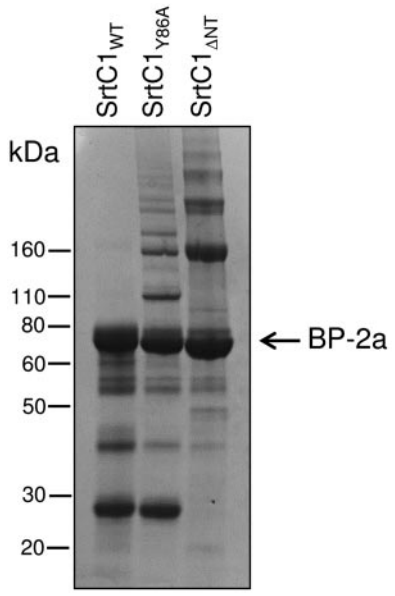

Figure 8. Mutant SrtC1 enzyme deleted of the entire N-terminal region is active in polymerizing BP-2a *in vitro*. SDS-PAGE analysis of the reactions performed *in vitro* between 100 μM of the recombinant BP-2a protein and 25 μM of $SrtC1_{WT}$, $SrtC1_{Y86A}$, and $SrtC1_{\Delta NT}$ after 72 h. A pattern of HMW structures could be identified only in the presence of $SrtC1_{Y86A}$ and $SrtC1_{\Delta NT}$.

observations, we performed *in vitro* experiments by using either the recombinant GBS $SrtC1_{WT}$ or the lid mutant $SrtC1_{Y86A}$ mixed with the purified recombinant BP-2a, carrying the sequence elements (as the pilin motif and the IPQTG sorting signal) absolutely required for pilus formation *in vivo*. We observed that, while the WT enzyme was totally inactive, the lid mutant $SrtC1_{Y86A}$ was able to efficiently assemble the backbone subunit in HMW polymers, clearly detectable by SDS-PAGE of the reaction mixtures and Coomassie staining. These data represent the first direct experimental evidence that a single residue in the lid can regulate the enzyme catalytic activity. However, we have previously observed that $SrtC1_{WT}$ is able to cleave the fluorogenic peptides carrying the LPXTG motifs of the substrate proteins in *in vitro* fluorescence resonance energy transfer (FRET)-based assays, probably because the used peptides are small enough to enter in the catalytic pocket (33, 34). The lid, interacting with the catalytic cysteine through a specific residue (*i.e.*, Tyr86 in GBS SrtC1-2a), blocks the enzyme in a closed conformation, thus preventing the accessibility to the substrate. The mutation of this key residue might break this interaction, making the active site available for substrate binding. Moreover, the elimination of the aromatic-sulfur interaction with the catalytic Cys219 side chain might induce a perturbation in the N-terminal flexible region (helix α1-α2) and/or increase the exposure of the β-barrel core to proteases. In fact, by biochemical characterization assays we observed that the presence of the lid in $SrtC1_{WT}$ confers to the enzyme stability and resistance to proteolysis. As observed in the proteolysis experiments, the β-barrel core becomes more susceptible to trypsin digestion when the Tyr86-Cys219 binding is absent and the active site is not protected by the lid. This observation leads to the hypothesis that the lid could be part of a prodomain, made of the entire N-terminal region, and that the activation of the enzyme might occur *via* proteolytic processing, producing an activated form consisting of the actual catalytic domain. In support of this hypothesis, we observed that the recombinant $SrtC1_{\Delta NT}$ mutant, lacking the entire N-terminal domain, still retains transpeptidation activity *in vitro* (Fig. 8), in accord with previous data showing that GBS pilus 1 SrtC mutants, deleted of the entire N terminus, are active in *in vitro* FRET-based assays (33). However, there is no direct evidence that the proteolytic removal of the N-terminal segment is the mechanism for SrtC enzyme activation on the bacterial surface, and our hypothesis needs to be validated. Certainly, our data are in agreement with the available structural data, which indicate that the conformation of the N-terminal segment is not compatible with substrate binding, implying that a conformational change that relocates the lid must occur in order to make the active-site groove accessible. Moreover, our data support the previously suggested hypothesis of SrtC enzymes having an N-terminal regulatory domain (including the lid region), not essential for enzyme catalysis, and a catalytic domain made by the β-barrel core (33). However, the function of the entire N-terminal domain must be further elucidated.

Another interesting finding shown in this work is that, in contrast to what is observed *in vivo* in native conditions, the $SrtC1_{Y86A}$ mutant can polymerize the pilus BP *in vitro* even when the lysine residue of the pilin motif is mutated. Therefore, we consider plausible the hypothesis that the flexible N-terminal domain, changing its conformation over the catalytic groove, could be involved both in the regulation of the enzyme activity and in the specific recognition of the pilin motif during the transpeptidation reaction. Also, we cannot exclude the possibility that additional factors on the bacterial surface could be involved in sortase activity regulation as well as in substrate specificity. Further efforts will be necessary to explore what exactly happens *in vivo* and to understand the differences at the molecular level between the catalytic mechanisms of transpeptidation occurring *in vitro vs. in vivo*. An additional open question is whether the regulation role played by the N-terminal domain, including the lid, is common for all pilus-related sortases, including those sortases that do not contain a canonical lid motif (30, 41).

Finally, another important message conveyed by this study regards the potential use of activated forms of pilus-associated sortases as a tool to elucidate the molecular basis of the SrtC-catalyzed transpeptidation reaction and characterize in more detail the polymeric structures. Pili play a key role in bacterial virulence/pathogenesis and are promising vaccine candidates, particularly in GBS, where they are present and well expressed on the surface of the majority of epidemio-

logically relevant clinical isolates (3). Hence, to study these proteins in their native form assembled in polymeric structures is surely of major scientific relevance. Currently, the only way to obtain pili structures is to develop laborious processes for purifying WT pili from pathogenic bacteria. Thus, the findings reported in this study offer a potentially novel strategy to produce *in vitro* recombinant polymeric complexes through easily implementable processes. However, to use the $SrtC1_{Y86A}$ mutant or similar derivatives, the characterization of pilus polymers is crucial, and the specificity of the catalytic mechanism of transpeptidation occurring *in vitro* needs to be further elucidated. FJ

This work was supported by the Joint Research Project 2010 between the University of Verona and Novartis Vaccines and Diagnostics (Siena, Italy). The authors thank Prof. Henriette Molinari for helpful discussions.

REFERENCES

1. Sendi, P., Johansson, L., and Norrby-Teglund, A. (2008) Invasive group B streptococcal disease in non-pregnant adults: a review with emphasis on skin and soft-tissue infections. *Infection* **36,** 100–111
2. Maione, D., Margarit, I., Rinaudo, C. D., Masignani, V., Mora, M., Scarselli, M., Tettelin, H., Brettoni, C., Iacobini, E. T., Rosini, R., D'Agostino, N., Miorin, L., Buccato, S., Mariani, M., Galli, G., Nogarotto, R., Dei, V. N., Vegni, F., Fraser, C., Mancuso, G., Teti, G., Madoff, L. C., Paoletti, L. C., Rappuoli, R., Kasper, D. L., Telford, J. L., and Grandi, G. (2005) Identification of a universal group B *Streptococcus* vaccine by multiple genome screen. *Science* **309,** 148–150
3. Margarit, I., Rinaudo, C. D., Galeotti, C. L., Maione, D., Ghezzo, C., Buttazzoni, E., Rosini, R., Runci, Y., Mora, M., Buccato, S., Pagani, M., Tresoldi, E., Berardi, A., Creti, R., Baker, C. J., Telford, J. L., and Grandi, G. (2009) Preventing bacterial infections with pilus-based vaccines: the group B *Streptococcus* paradigm. *J. Infect. Dis.* **199,** 108–115
4. Mandlik, A., Swierczynski, A., Das, A., and Ton-That, H. (2008) Pili in gram-positive bacteria: assembly, involvement in colonization and biofilm development. *Trends Microbiol.* **16,** 33–40
5. Manetti, A. G., Zingaretti, C., Falugi, F., Capo, S., Bombaci, M., Bagnoli, F., Gambellini, G., Bensi, G., Mora, M., Edwards, A. M., Musser, J. M., Graviss, E. A., Telford, J. L., Grandi, G., and Margarit, I. (2007) *Streptococcus* pyogenes pili promote pharyngeal cell adhesion and biofilm formation. *Mol. Microbiol.* **64,** 968–983
6. Pezzicoli, A., Santi, I., Lauer, P., Rosini, R., Rinaudo, D., Grandi, G., Telford, J. L., and Soriani, M. (2008) Pilus backbone contributes to group B *Streptococcus* paracellular translocation through epithelial cells. *J. Infect. Dis.* **198,** 890–898
7. Rinaudo, C. D., Rosini, R., Galeotti, C. L., Berti, F., Necchi, F., Reguzzi, V., Ghezzo, C., Telford, J. L., Grandi, G., and Maione, D. (2010) Specific involvement of pilus type 2a in biofilm formation in group B *Streptococcus*. *PloS One* **5,** e9216
8. Dramsi, S., Caliot, E., Bonne, I., Guadagnini, S., Prevost, M. C., Kojadinovic, M., Lalioui, L., Poyart, C., and Trieu-Cuot, P. (2006) Assembly and role of pili in group B streptococci. *Mol. Microbiol.* **60,** 1401–1413
9. Rosini, R., Rinaudo, C. D., Soriani, M., Lauer, P., Mora, M., Maione, D., Taddei, A., Santi, I., Ghezzo, C., Brettoni, C., Buccato, S., Margarit, I., Grandi, G., and Telford, J. L. (2006) Identification of novel genomic islands coding for antigenic pilus-like structures in *Streptococcus agalactiae*. *Mol. Microbiol.* **61,** 126–141
10. Schneewind, O., and Missiakas, D. M. (2012) Protein secretion and surface display in gram-positive bacteria. *Philos. Trans. R. Soc. Lond. B Biol. Sci.* **367,** 1123–1139
11. Vengadesan, K., Ma, X., Dwivedi, P., Ton-That, H., and Narayana, S. V. (2011) A model for group B *Streptococcus* pilus type 1: the structure of a 35-kDa C-terminal fragment of the major pilin GBS80. *J. Mol. Biol.* **407,** 731–743
12. Necchi, F., Nardi-Dei, V., Biagini, M., Assfalg, M., Nuccitelli, A., Cozzi, R., Norais, N., Telford, J. L., Rinaudo, C. D., Grandi, G., and Maione, D. (2011) Sortase A substrate specificity in GBS pilus 2a cell wall anchoring. *PloS One* **6,** e25300
13. Nobbs, A. H., Rosini, R., Rinaudo, C. D., Maione, D., Grandi, G., and Telford, J. L. (2008) Sortase A utilizes an ancillary protein anchor for efficient cell wall anchoring of pili in *Streptococcus agalactiae*. *Infect. Immunity* **76,** 3550–3560
14. Telford, J. L., Barocchi, M. A., Margarit, I., Rappuoli, R., and Grandi, G. (2006) Pili in gram-positive pathogens. *Nat. Rev. Microbiology* **4,** 509–519
15. Ton-That, H., Marraffini, L. A., and Schneewind, O. (2004) Protein sorting to the cell wall envelope of gram-positive bacteria. *Biochimica et Biophysica Acta* **1694,** 269–278
16. Ton-That, H., Marraffini, L. A., and Schneewind, O. (2004) Sortases and pilin elements involved in pilus assembly of *Corynebacterium diphtheriae*. *Mol. Microbiol.* **53,** 251–261
17. Hendrickx, A. P., Budzik, J. M., Oh, S. Y., and Schneewind, O. (2011) Architects at the bacterial surface - sortases and the assembly of pili with isopeptide bonds. *Nat. Rev. Microbiology* **9,** 166–176
18. Ilangovan, U., Ton-That, H., Iwahara, J., Schneewind, O., and Clubb, R. T. (2001) Structure of sortase, the transpeptidase that anchors proteins to the cell wall of *Staphylococcus aureus*. *Proc. Natl. Acad. Sci. U. S. A.* **98,** 6056–6061
19. Marraffini, L. A., Ton-That, H., Zong, Y., Narayana, S. V., and Schneewind, O. (2004) Anchoring of surface proteins to the cell wall of *Staphylococcus aureus*. A conserved arginine residue is required for efficient catalysis of sortase A. *J. Biol. Chem.* **279,** 37763–37770
20. Ton-That, H., Mazmanian, S. K., Alksne, L., and Schneewind, O. (2002) Anchoring of surface proteins to the cell wall of *Staphylococcus aureus*. Cysteine 184 and histidine 120 of sortase form a thiolate-imidazolium ion pair for catalysis. *J. Biol. Chem.* **277,** 7447–7452
21. Ton-That, H., Mazmanian, S. K., Faull, K. F., and Schneewind, O. (2000) Anchoring of surface proteins to the cell wall of *Staphylococcus aureus*. Sortase catalyzed in vitro transpeptidation reaction using LPXTG peptide and NH(2)-Gly(3) substrates. *J. Biol. Chem.* **275,** 9876–9881
22. Zong, Y., Bice, T. W., Ton-That, H., Schneewind, O., and Narayana, S. V. (2004) Crystal structures of *Staphylococcus aureus* sortase A and its substrate complex. *J. Biol. Chem.* **279,** 31383–31389
23. Budzik, J. M., Oh, S. Y., and Schneewind, O. (2008) Cell wall anchor structure of BcpA pili in *Bacillus anthracis*. *J. Biol. Chem.* **283,** 36676–36686
24. Marraffini, L. A., Dedent, A. C., and Schneewind, O. (2006) Sortases and the art of anchoring proteins to the envelopes of gram-positive bacteria. *Microbiol. Mol. Biol. Rev.* **70,** 192–221
25. Neiers, F., Madhurantakam, C., Falker, S., Manzano, C., Dessen, A., Normark, S., Henriques-Normark, B., and Achour, A. (2009) Two crystal structures of pneumococcal pilus sortase C provide novel insights into catalysis and substrate specificity. *J. Mol. Biol.* **393,** 704–716
26. Spirig, T., Weiner, E. M., and Clubb, R. T. (2011) Sortase enzymes in Gram-positive bacteria. *Mol. Microbiol.* **82,** 1044–1059
27. Manzano, C., Contreras-Martel, C., El Mortaji, L., Izore, T., Fenel, D., Vernet, T., Schoehn, G., Di Guilmi, A. M., and Dessen, A. (2008) Sortase-mediated pilus fiber biogenesis in *Streptococcus pneumoniae*. *Structure* **16,** 1838–1848
28. Manzano, C., Izore, T., Job, V., Di Guilmi, A. M., and Dessen, A. (2009) Sortase activity is controlled by a flexible lid in the pilus biogenesis mechanism of gram-positive pathogens. *Biochemistry* **48,** 10549–10557
29. Persson, K. (2011) Structure of the sortase AcSrtC-1 from *Actinomyces oris*. *Acta Crystallogr. D Biolog. Crystallogr.* **67,** 212–217
30. Lu, G., Qi, J., Gao, F., Yan, J., Tang, J., and Gao, G. F. (2011) A novel "open-form" structure of sortase C from *Streptococcus suis*. *Proteins* **79,** 2764–2769
31. Khare, B., Fu, Z. Q., Huang, I. H., Ton-That, H., and Narayana, S. V. (2011) The crystal structure analysis of group B *Streptococcus* sortase C1: a model for the "lid" movement upon substrate binding. *J. Mol. Biol.* **414,** 563–577

32. Khare, B., Krishnan, V., Rajashankar, K. R., H, I. H., Xin, M., Ton-That, H., and Narayana, S. V. (2011) Structural differences between the *Streptococcus agalactiae* housekeeping and pilus-specific sortases: SrtA and SrtC1. *PloS One* **6,** e22995
33. Cozzi, R., Prigozhin, D., Rosini, R., Abate, F., Bottomley, M. J., Grandi, G., Telford, J. L., Rinaudo, C. D., Maione, D., and Alber, T. (2012) Structural basis for group B streptococcus pilus 1 sortases C regulation and specificity. *PloS One* **7,** e49048
34. Cozzi, R., Malito, E., Nuccitelli, A., D'Onofrio, M., Martinelli, M., Ferlenghi, I., Grandi, G., Telford, J. L., Maione, D., and Rinaudo, C. D. (2011) Structure analysis and site-directed mutagenesis of defined key residues and motives for pilus-related sortase C1 in group B *Streptococcus*. *FASEB J.* **25,** 1874–1886
35. Wu, C., Mishra, A., Reardon, M. E., Huang, I. H., Counts, S. C., Das, A., and Ton-That, H. (2012) Structural determinants of *Actinomyces* sortase SrtC2 required for membrane localization and assembly of type 2 fimbriae for interbacterial coaggregation and oral biofilm formation. *J. Bacteriol.* **194,** 2531–2539
36. Klock, H. E., and Lesley, S. A. (2009) The polymerase incomplete primer extension (PIPE) method applied to high-throughput cloning and site-directed mutagenesis. *Methods Mol. Biol.* **498,** 91–103
37. Nuccitelli, A., Cozzi, R., Gourlay, L. J., Donnarumma, D., Necchi, F., Norais, N., Telford, J. L., Rappuoli, R., Bolognesi, M., Maione, D., Grandi, G., and Rinaudo, C. D. (2011) Structure-based approach to rationally design a chimeric protein for an effective vaccine against group B *Streptococcus* infections. *Proc. Natl. Acad. Sci. U. S. A.* **108,** 10278–10283
38. Ericsson, U. B., Hallberg, B. M., Detitta, G. T., Dekker, N., and Nordlund, P. (2006) Thermofluor-based high-throughput stability optimization of proteins for structural studies. *Anal. Biochem.* **357,** 289–298
39. Sklenar, V. B., A (1987) Spin-echo water suppression for the generation of pure-phase two-dimensional NMR spectra. *J. Magn. Res.* **74,** 469–479
40. Cozzi, R., Nuccitelli, A., D'Onofrio, M., Necchi, F., Rosini, R., Zerbini, F., Biagini, M., Norais, N., Beier, C., Telford, J. L., Grandi, G., Assfalg, M., Zacharias, M., Maione, D., and Rinaudo, C. D. (2012) New insights into the role of the glutamic acid of the E-box motif in group B *Streptococcus* pilus 2a assembly. *FASEB J.* **26,** 2008–2018
41. Kang, H. J., Coulibaly, F., Proft, T., and Baker, E. N. (2011) Crystal structure of Spy0129, a *Streptococcus pyogenes* class B sortase involved in pilus assembly. *PloS One* **6,** e15969

Received for publication January 15, 2013.
Accepted for publication April 15, 2013.